Rashba spin-orbital splitting in quantum anti-wires

A. M. BABAYEV[a,b], Ş. ÇAKMAKTEPE[c], D. T. ALTUG[a]
[a]*Department of Physics, University of Suleyman Demirel, Isparta 32260, Turkey*
[b]*Institute of Physics, Azerbaijan Academy of Sciences, 370143, Baku, Azerbaijan*
[c]*Department of Physics, Kilis 7 Aralik University, Kilis, Turkey.*

The electronic states of a semiconductor quantum-antiwire in the presence of Rashba spin-orbital interaction and external magnetic field are theoretically investigated taking into account the simple parabolic band model. Calculations are performed for a hard-wall confinement potential. The radii, height, coupling strength and magnetic field dependence of Rashba splitting are calculated for electrons. It has been found that Rashba splitting of electrons are decreased with the increasing of anti-wire's radius and thickness.

(Received February 28, 2009; accepted May 26, 2009)

Keywords: Spintronics, Rashba spin splitting, Quantum anti-wire

1. Introduction

There has been an explosive interest both experimental and theoretical points of semiconductor nanocrystals in recent years [1]. The interest concentrates on an ultimate limit of size quantization in solids in those objects. Most of it is focused on spin-related optical and transport properties of low dimensional semiconductor structures. Spin orbital interactions can arise in quantum dots by various mechanisms related to electron confinement and symmetry breaking and are generally introduced into Hamiltonian via the Rashba [2] and Dresselhauss terms [3]. It was shown by Dresselhauss that in bulk semiconductors of zinc blende symmetry, the Γ6 band (conduction band of III-V compounds) is characterized by an anisotropic spin splitting proportional to k3 for small k values. The splitting was extensively investigated in bulk semiconductors with the use of optical and transport methods. In particular, the splitting leads to electron spin relaxation, as demonstrated by Dynakov and Perel [4]. The use of the Rashba interaction to controllably rotate the electron spin was first proposed by Datta and Das [5]. Using this earlier proposal and its potential applications on semiconductor spintronics, many researchers are actively investigating spin-orbit related physics of different semiconductor nanostructures. The first theoretical study in the spin splitting of conduction band in semiconductor heterostructures is done by Okava and Uemura [6]. Lassnig was the first to recognize the essential point that the spin inversion asymmetry splitting in the conduction band is related to the gradient of the potential including the valance offsets at the interfaces [7]. Pfeffer and Zawadski used the complete five level k.p approach to the band structure of III-V compounds, which allowed to treat bulk inversion asymmetry and structure inversion asymmetry mechanism of spin-splitting within the same model [8]. In [9,10], analytic solutions to the problem of the Rashba spin-orbit coupling were done in semiconductor quantum dots. The energy spectrum, wave functions and spin-flip relaxation times were calculated using perturbation theory. The above descriptions treat the case of a simple parabolic energy band. Hashimzade et al were considered theoretically the electrons in Kane type semiconductor quantum disk in presence of Rashba spin orbital interaction and external magnetic field parallel to the axis of quantum disk [11]. Kudryashov were calculated the Rashba spin orbit interaction, wave functions and energy spectrum in a two dimensional quantum dot [12].

In the present study, it's calculated the total spin-splitting energy in an InSb quantum anti-wire with hard walls both without and with an applied constant axial magnetic field taking into account the simple parabolic band model. It has a contribution due to the Zeeman Effect and another to the Rashba effect. The system considered here might simply be a very long cylindrical

cavity of radius R etched out of a bulk composite semiconductor material. The structure thought of here is therefore the one-dimensional analogue of the two-dimensional hetero-junction or electric potential barrier. An alternative design would be to have a superconducting core enveloped in a semiconductor matrix. This would constitute a cylindrical magnetic barrier or if the length and the radius of the core are comparable, a magnetic antidot [13]. It's shown an example of an anti-wire in Figure 1 [14]. Every cavity in Figure 1 corresponds to an anti-wire. The whole figure is called as photonic crystals which are now envisaged as an essential building of future photonic devices [15].

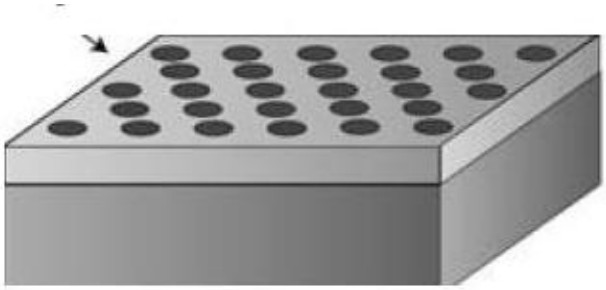

Fig. 1. Anti-wire example.

2. Zero Magnetic Field

In the simple parabolic band model, the solution of the Shrödinger equation is investigated by adding Rashba spin-orbit splitting term to the Schrödinger equation. We describe the confinement of electrons in quantum anti-wire by a separable potential V(r)=V(z) +V(x, y), where V(x, y) is the confinement potential in the xy plane and V(z) is the potential in the z direction. The confining potential in the xy plane is assumed to be symmetric, V(x, y)= $V(\rho)$. Here we will mainly consider a hard-wall confining potential in the xy plane, $V(\rho)=0$ for $\rho > r_0$ and $V(\rho)=\infty$ for $\rho = r_0$, r_0 being the radius of the quantum anti-wire. The perpendicular confinement V(z) is assumed strong enough that only the lowest z-subband is occupied. Here V(z) is assumed to be asymmetric.

The Hamiltonian of the Schrödinger equation for the electrons of quantum anti-wire is described as;

$$H = \frac{p^2}{2m} + V(x,y,z) + \alpha_R(k_x\sigma_y - k_y\sigma_x) + \frac{1}{2}g\mu_B B\sigma_z \tag{1}$$

where m is the effective mass, αR is the Rashba spin-orbital splitting term, μB is the Bohr magneton, $\vec{\sigma} = (\sigma_x, \sigma_y, \sigma_z)$ is the Pauli spin matrices and B is the magnetic field parallel to the z axis. Firstly we are going to be focused on the zero magnetic fields, so B will be taken as zero.
Spin splitting in heterostructures is occurred by the asymmetric confinement potential and is shown by Rashba Hamiltonian;

$$H_R = \alpha_R(k_x\sigma_y - k_y\sigma_x) \tag{2}$$

The confinement potential is assumed to be symmetric. The Schrödinger equation will be written as;

$$\left(\frac{p^2}{2m} + V(x,y) + H_R\right)\psi = E\psi \tag{3}$$

In this paper, we mainly consider a hard-wall confining potential, the potential of the quantum anti-wire to be infinitive and consequently the wave functions to be zero at the boundary. The

perturbation theory is applied by accepting the Rashba spin-orbital interaction term as weak perturbation term. After averaging in the z direction, for the lowest subband, we obtain the following set of two equations for the envelopes $\psi_1(r)$ and $\psi_2(r)$:

$$\begin{cases} \frac{\hbar^2(\hat{k}_x^2+\hat{k}_y^2+<\hat{k}_z^2>)}{2m}-E)\psi_1-i\alpha_R\hat{k}_-\psi_2=0 \\ i\alpha_R\hat{k}_+\psi_1+\frac{\hbar^2(\hat{k}_x^2+\hat{k}_y^2+<\hat{k}_z^2>)}{2m}-E)\psi_2=0 \end{cases} \tag{4}$$

is obtained, where $<\hat{k}_z^2>\approx\frac{\pi^2}{d^2}$ where d is the confinement length in the z direction [16] and operators $\hat{k}_\pm$ in cylindrical coordinates take the form;

$$\hat{k}_\pm=-ie^{\pm i\varphi}(\frac{d}{d\rho}\pm\frac{i}{\rho}\frac{d}{d\varphi}) \tag{5}$$

We consider a quantum anti-wire modeled as a quantum cylindrical cavity of radius r0 etched out of a bulk composite semiconductor material and the thickness d. Because of the symmetry of the problem it is convenient to use cylindrical coordinates (ρ,φ)

The eigenfunctions of the total momentum operator with a half integer eigenvalue j, are of the following form;

$$\psi_j(\rho,\varphi)=\begin{bmatrix} e^{i(j-1/2)\varphi}f_j(\rho) \\ e^{i(j+1/2)\varphi}g_j(\rho) \end{bmatrix} \tag{6}$$

where j=0, ±1/2, ±3/2, ±5/2, ... are the magnetic quantum numbers.

The spinor components in equation (6) satisfy the following system of second-order ordinary differential equations;

$$-\frac{\hbar^2}{2m}\left[\left(\frac{1}{\rho}\frac{d}{d\rho}\left(\rho\frac{d}{d\rho}\right)\right)-\frac{(j-1/2)^2}{\rho^2}\right]f(\rho)-\alpha_R\left[\frac{d}{d\rho}+\frac{j+1/2}{\rho}\right]g(\rho) \tag{7}$$
$$=\left(E-\frac{\hbar^2}{2m}\frac{\pi^2}{d^2}\right)f(\rho)$$

$$-\frac{\hbar^2}{2m}\left[\left(\frac{1}{\rho}\frac{d}{d\rho}\left(\rho\frac{d}{d\rho}\right)\right)-\frac{(j-1/2)^2}{\rho^2}\right]f(\rho)+\alpha_R\left[\frac{d}{d\rho}-\frac{j+1/2}{\rho}\right]f(\rho) \tag{8}$$
$$=\left(E-\frac{\hbar^2}{2m}\frac{\pi^2}{d^2}\right)g(\rho)$$

Then the wave functions are taken as Bessel functions;

$$f(\rho)=d_1Y_{j-1/2}(k\rho)\quad g(\rho)=d_2Y_{j+1/2}(k\rho) \tag{9}$$

If it's taken into account the following equations for Bessel functions;

$$\left(\frac{d}{dx}+\frac{j+1/2}{x}\right)Y_{j+1/2}(kx)=kY_{j-1/2}(kx) \tag{10}$$

$$\left(\frac{d}{dx}+\frac{j-1/2}{x}\right)Y_{j-1/2}(kx)=kY_{j+1/2}(kx) \tag{11}$$

$$\left(\frac{d^2}{d\rho^2}+\frac{1}{\rho}\frac{d}{d\rho}-\frac{m^2}{\rho^2}+k^2\right)Y_m(k\rho)=0 \tag{12}$$

Equations (7) and (8) can be written as;

$$\left(-k^2+\frac{2mE}{\hbar^2}-\frac{\pi^2}{d^2}\right)d_1+k\frac{2m\alpha_R}{\hbar^2}d_2=0 \tag{13}$$

$$\left(-k^2+\frac{2mE}{\hbar^2}-\frac{\pi^2}{d^2}\right)d_2+k\frac{2m\alpha_R}{\hbar^2}d_1=0 \tag{14}$$

the solutions of the above equations are;

$$\begin{vmatrix} \frac{2mE}{\hbar^2}-\frac{\pi^2}{d^2}-k^2 & k\frac{2m\alpha_R}{\hbar^2} \\ k\frac{2m\alpha_R}{\hbar^2} & \frac{2mE}{\hbar^2}-\frac{\pi^2}{d^2}-k^2 \end{vmatrix}=0 \tag{15}$$

From the equation (15) it's taken,

$$\left(\frac{2mE}{\hbar^2}-\frac{\pi^2}{d^2}-k^2\right)^2-k^2\left(\frac{2m\alpha_R}{\hbar^2}\right)^2=0 \tag{16}$$

If the equation (16) is solved for the k then

$$k_{1+}=\pm\frac{1}{2}\frac{2m\alpha_R}{\hbar^2}+\sqrt{\frac{2mE}{\hbar^2}-\frac{\pi^2}{d^2}+\frac{1}{4}\left(\frac{2m\alpha_R}{\hbar^2}\right)^2}, \qquad k_{2+}=\pm\frac{1}{2}\frac{2m\alpha_R}{\hbar^2}\pm\sqrt{\frac{2mE}{\hbar^2}-\frac{\pi^2}{d^2}+\frac{1}{4}\left(\frac{2m\alpha_R}{\hbar^2}\right)^2} \tag{17}$$

are obtained.

The ratio of d1 and d2 constants convenient for the $k_{1\pm}$ values is as follows:

$$\frac{d_1^+}{d_2^+}=-\frac{\frac{2m\alpha_R}{\hbar^2}k_{1+}}{\frac{2mE}{\hbar^2}-\frac{\pi^2}{d^2}-k_{1+}^2}, \frac{d_1^-}{d_2^-}=-\frac{\frac{2mE}{\hbar^2}-\frac{\pi^2}{d^2}-k_{1-}^2}{\frac{2m\alpha_R}{\hbar^2}k_{1-}} \tag{18}$$

Hence there are two degenerate solutions for $k_{\pm}$ that are combined in the general solution

$$\begin{bmatrix} f_j(x) \\ g_j(x) \end{bmatrix}=A\begin{bmatrix} d_1^+Y_{j-1/2}(k_{1+}x) \\ d_2^+Y_{j+1/2}(k_{1+}x) \end{bmatrix}+B\begin{bmatrix} d_1^-Y_{j-1/2}(k_{1-}x) \\ d_2^-Y_{j+1/2}(k_{1-}x) \end{bmatrix} \tag{19}$$

We imply the Drichlet boundary condition as x=r for k linear combination of solution (19)

$$\begin{bmatrix} d_1^+Y_{j-1/2}(k_{1+}x)\ d_1^-Y_{j-1/2}(k_{1-}x) \\ d_2^+Y_{j+1/2}(k_{1+}x)\ d_2^-Y_{j+1/2}(k_{1-}x) \end{bmatrix}\begin{bmatrix} A \\ B \end{bmatrix}=0 \tag{20}$$

It gives us the following exact equation for energy spectrum of the quantum anti-wire with spin orbital interacting

$$\frac{d_1^+}{d_2^+}\frac{d_2^-}{d_1^-}Y_{j-1/2}(k_{1+})Y_{j+1/2}(k_{1-})-Y_{j-1/2}(k_{1-})Y_{j+1/2}(k_{1+})=0 \tag{21}$$

For value of $k_{1\pm}$ $\frac{d_1^+}{d_2^+}\frac{d_2^-}{d_1^-}=-1$ equation (21) simplifies to

$$Y_{j-1/2}(k_{1+}\rho)Y_{j+1/2}(k_{1-}\rho)+Y_{j-1/2}(k_{1-}\rho)Y_{j+1/2}(k_{1+}\rho)=0 \tag{22}$$

The n th solution of equation (22), is shown the n th energy level of the electron which have a momentum of j+1/2.
Equation (22) is invariant under the change j→-j which reflects the Kramer's degeneracy. At α=0, all states with l≠0 are fourfold degenerate, while l=0 states are doubly degenerate. According to the standard analysis the spin-orbit coupling splits all the l≠0 states into two Kramers doublets with j=l+1/2 and j=l-1/2, while l=0 states naturally remain Kramer's doublets.
We have analyzed Equation (22) numerically, labeling the energy eigenstates as (j,n) where n is a non-negative integer such that Ej,n<Ej,n+1 at αR=0. The evolution of the first few energy levels with the parameter α is shown in Figure 5.
So, the eigenvalues and eigenfunctions of the obtained two-dimensional Hamiltonian are found. Then with the help of the boundary condition in which the eigenfunctions are equal to zero at the boundary of the quantum anti-wire, the energy spectrum of electrons is obtained. The radii dependence of the Rashba spin-orbit splitting is plotted in Figure 2, while the radii and height dependence of the energies are plotted in Figure 3 and Figure 4 respectively in a quantum anti-wire.

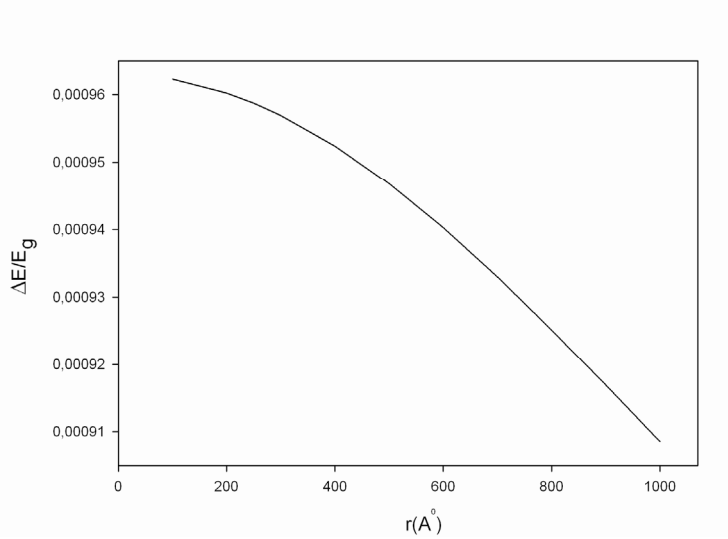

Fig. 2. The change of Rashba spin-orbit splitting in InSb quantum anti-wire for the states of (1/2,1) -(3/2,0) (B=0).

In Figure 2, it's shown the radii dependence of Rashba spin-orbit splitting in quantum anti-wire. As it's seen from the Figure 2, the value of the Rashba spin-splitting is decreasing with the increasing of the radius.

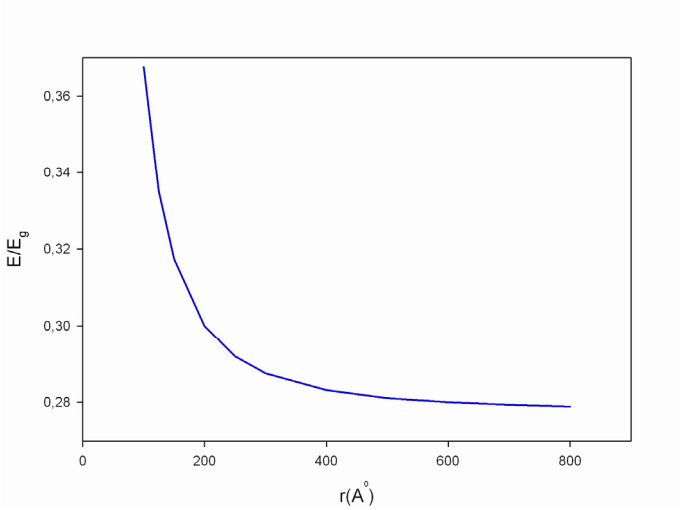

Fig. 3. The radii dependence of electron energies in InSb quantum anti-wire for the states of (1/2,0).

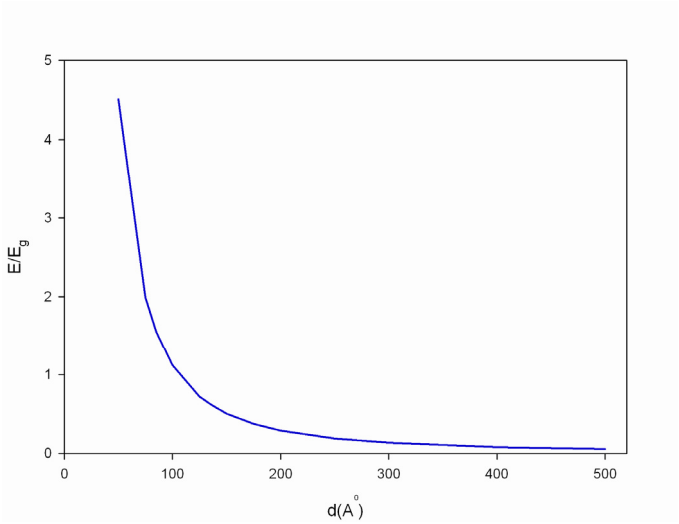

Fig. 4. The height dependence of electron energies in InSb quantum anti-wire for the states of (1/2,0). (r=300 Å)

In Figure 3 and 4, the radius and height dependence of electron energies in InSb quantum anti-wire, are shown where Rashba parameter is constant. It's seen from the Figures 3 and 4 that the energies are decreasing with the increasing of radius and thickness.

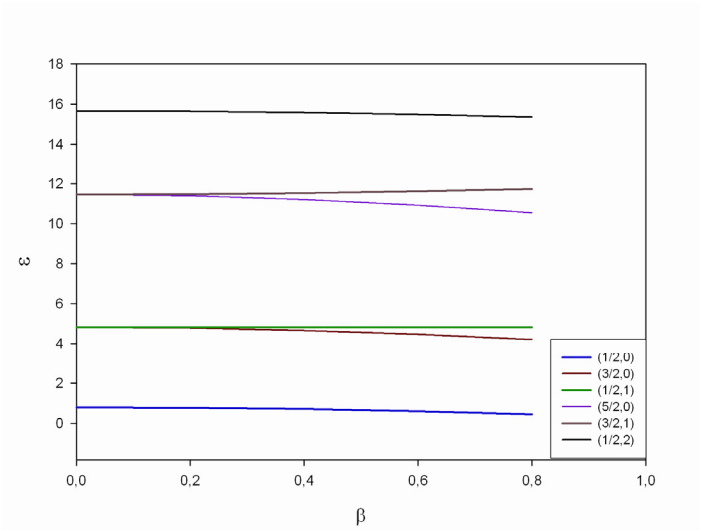

Fig. 5. The Rashba parameter change of electron energies in InSb quantum anti-wire (B=0).

$$\beta = \frac{2m\alpha_R}{\hbar^2}\rho,\ \varepsilon = \frac{2mE}{\hbar^2}\rho^2 - \rho^2\frac{\pi^2}{d^2}$$

It's seen the Rashba parameter dependence of electron energies in Figure 5. For the quantum sates ($J=1/2,\ \ n=1$) and ($J=3/2,\ \ n=0$) the Rashba splitting is observed while for the ground state ($J=1/2,\ \ n=0$) it couldn't find spin-orbit splitting due to Rashba parameter.

3. Applied Magnetic Field

In the second case the problem is solved under an applied magnetic field. For a uniform magnetic field H, directed along the z-axis, the vector potential may be chosen in the form;

$$\vec{A}=\left(-\frac{Hy}{2},\frac{Hx}{2},0\right) \tag{23}$$

the operators k± in Eqs. (15) and (16) become cylindrical coordinates and take the form

$$k_{\pm}=-i\exp(\pm i\varphi)\left(\frac{\partial}{\partial\rho}\pm\frac{i}{\rho}\frac{\partial}{\partial\varphi}\pm\frac{\rho}{2\alpha^2}\right) \tag{24}$$

where $\alpha=\sqrt{\frac{\hbar c}{eH}}$ is the magnetic length. Since the system is cylindrically symmetric, the wave function can be represented as [19];

$$\begin{pmatrix}\varphi_1\\ \varphi_2\end{pmatrix}=\begin{pmatrix}\exp(im\varphi)\exp\left(-\frac{x}{2}\right)x^{|m|/2}Y(x)\\ \exp(i(m+1)\varphi)\exp\left(-\frac{x}{2}\right)x^{|m+1|/2}Z(x)\end{pmatrix} \tag{25}$$

where; $x=\frac{\rho^2}{2\alpha^2}$.

By using the formulas of (23) and (24), we obtain second order differential equations for the radial functions;

$$x\frac{d^2Y(x)}{dx^2}+(|m|-x+1)\frac{dY(x)}{dx}-\frac{1}{2}(1+|m|+m-k_t^2\alpha^2-h\alpha^2)Y(x)+\frac{1}{\sqrt{2}}x^{\frac{1}{2}+\frac{|m+1|-|m|}{2}}\beta\alpha\frac{dZ(x)}{dx}$$
$$+\frac{\alpha\beta x^{-\frac{1}{2}+\frac{|m+1|-|m|}{2}}}{2\sqrt{2}}(1+m+|m+1|)Z(x)=0 \tag{26}$$

$$x\frac{d^2Z(x)}{dx^2}+(|m+1|-x+1)\frac{dZ(x)}{dx}-\frac{1}{2}(2+|m+1|+m-k_t^2\alpha^2+h\alpha^2)Z(x)$$
$$-\frac{1}{\sqrt{2}}x^{\frac{1}{2}+\frac{|m|-|m+1|}{2}}\beta\alpha\frac{dY(x)}{dx}-\frac{\alpha\beta x^{-\frac{1}{2}+\frac{|m|-|m+1|}{2}}}{2\sqrt{2}}(|m|-m-2x)Y(x)=0 \tag{27}$$

In Equations (26) and (27) the following notations are used;

$$\alpha=\sqrt{\frac{\hbar c}{eB}},\frac{2m}{\hbar}\alpha_R=\beta_R,k_t^2=\frac{2mE}{\hbar^2}-\frac{\pi^2}{d^2},\quad \hbar\alpha^2=-\frac{gm_n}{2m_0}$$, gInSb=-51

Let us introduce a_1 and a_2 parameters which are related to the equation in the following form:

$$x\frac{d^2Y(x)}{dx^2}+\left(-x+1+|m|\right)\frac{dY(x)}{dx}-a_1Y(x)=0 \tag{28}$$

$$x\frac{d^2Z(x)}{dx^2}+\left(-x+1+|m|+1\right)\frac{dZ(x)}{dx}-a_2Z(x)=0 \tag{29}$$

The equations are canonical form of Kummer's equations for the confluent hypergeometric function [20]. Equation (26) and (27) can be written as follows taking into account the equations of (28) and (29).

$$\left(a_1-\frac{1}{2}(1+|m|+m-k_t^2\alpha^2-h\alpha^2)\right)Y(x)+\frac{1}{\sqrt{2}}x^{\frac{1}{2}+\frac{|m+1|-|m|}{2}}\beta\alpha\frac{dZ(x)}{dx}$$
$$+\frac{\alpha\beta x^{-\frac{1}{2}+\frac{|m+1|-|m|}{2}}}{2\sqrt{2}}(1+m+|m+1|)Z(x)=0 \tag{30}$$

$$\left(a_2-\frac{1}{2}(2+|m+1|+m-k_t^2\alpha^2+h\alpha^2)\right)Z(x)$$
$$-\frac{1}{\sqrt{2}}x^{\frac{1}{2}+\frac{|m|-|m+1|}{2}}\beta\alpha\frac{dY(x)}{dx}-\frac{\alpha\beta x^{-\frac{1}{2}+\frac{|m|-|m+1|}{2}}}{2\sqrt{2}}(|m|-m-2x)Y(x)=0 \tag{31}$$

The solutions of Equations (30) and (31) that is bounded is $Y(x) = d_1 U(a_1, b_1, x)$ and $Z(x) = d_2 U(a_2, b_2, x)$, where

$$a_1 = \frac{m+|m|}{2} - \varepsilon_{0\pm}, \quad b_1 = |m| + 1 \tag{32}$$

$$a_2 = \frac{m+1+|m+1|}{2} - 1 - \varepsilon_{0\pm}, \quad b_2 = |m+1| + 1 \tag{33}$$

$$\varepsilon_{0\pm} = \frac{1}{2}(-2 + \frac{1}{2}\alpha^2\beta_R^2 + \alpha^2 k_t^2 \pm \sqrt{1 + 2h\alpha^2 + 4(h\alpha^2)^2 + \frac{1}{4}\alpha^4\beta_R^4 + \alpha^4\beta_R^2 k_t^2} \tag{34}$$

The wave function can be written;

$$R^+(x) = c_1 d_{1+} U\left(\frac{m+|m|}{2} - 1 - \varepsilon_{0+}, b_1, x\right) + c_2 d_{2+} U\left(\frac{m+1+|m+1|}{2} - 1 - \varepsilon_{0+}, b_2, x\right) \tag{35}$$

$$R^-(x) = c_1 d_{1-} U\left(\frac{m+|m|}{2} - 1 - \varepsilon_{0-}, b_1, x\right) + c_2 d_{2-} U\left(\frac{m+1+|m+1|}{2} - 1 - \varepsilon_{0-}, b_2, x\right) \tag{36}$$

In a nano anti-wire with an infinite potential barrier, the wave function must vanish at the quantum anti-wire's surface giving the dispersion equation for the electron quantum size levels:

$$\frac{d_{1+}}{d_{1-}}\frac{d_{2-}}{d_{2+}} \begin{pmatrix} U\left(\frac{m+|m|}{2} - 1 - \varepsilon_{0+}, b_1, x\right) + U\left(\frac{m+1+|m+1|}{2} - 1 - \varepsilon_{0-}, b_2, x\right) \\ -U\left(\frac{m+|m|}{2} - 1 - \varepsilon_{0-}, b_1, x\right) + U\left(\frac{m+1+|m+1|}{2} - 1 - \varepsilon_{0+}, b_2, x\right) \end{pmatrix} \tag{37}$$

where

$$\frac{d_{1+}d_{2-}}{d_{1-}d_{2+}} = \frac{\sqrt{1+\varepsilon_{0+}}}{\sqrt{1+\varepsilon_{0-}}} \frac{-\varepsilon_{0-} - \frac{1}{2}\left(1 - h\alpha^2 - \alpha^2 k_t^2\right)}{-\varepsilon_{0+} - \frac{1}{2}\left(1 - h\alpha^2 - \alpha^2 k_t^2\right)} \tag{38}$$

The above equation provides all information about the energy spectrum of electrons. The energy is a complicated function of the anti-wire parameters ρ, d and the electron angular momentum. Equation (37) can be useful for analyzing the influence of nonparabolicity on the energy spectrum of electrons near a quantum anti-wire.

We consider a disk with radius ρ and the height d in the cylindrical coordinates (ρ, φ, z). Then if it's applied the calculations of the study of [9, 11] for the quantum anti-wire, one can find the quantized energy levels of electrons in a quantum anti-wire by the following equation;

$$\frac{\sqrt{1+\varepsilon_{0+}}}{\sqrt{1+\varepsilon_{0-}}} \frac{-\varepsilon_{0-} - \frac{1}{2}\left(1 - h\alpha^2 - \alpha^2 k_z^2\right)}{-\varepsilon_{0+} \frac{1}{2}\left(1 - h\alpha^2 - \alpha^2 k_z^2\right)} = \frac{U\left[\frac{m+|m|}{2} - \varepsilon_{0-}, 1+|m|, x\right] U\left[\frac{m+1+|m+1|}{2} - \varepsilon_{0+} - 1, 1+|m+1|, x\right]}{U\left[\frac{m+|m|}{2} - \varepsilon_{0+}, 1+|m|, x\right] U\left[\frac{m+1+|m+1|}{2} - \varepsilon_{0-} - 1, 1+|m+1|, x\right]} \tag{39}$$

Equation (39) provides all the information about the energy spectrum of electrons. The energy is a complicated function of the disk parameters ρ, d and the electron angular momentum m. The energy system consists of discrete levels enumerated by a set of numbers {n,m}, where n denotes the nth solution of equation (39) with fixed m.

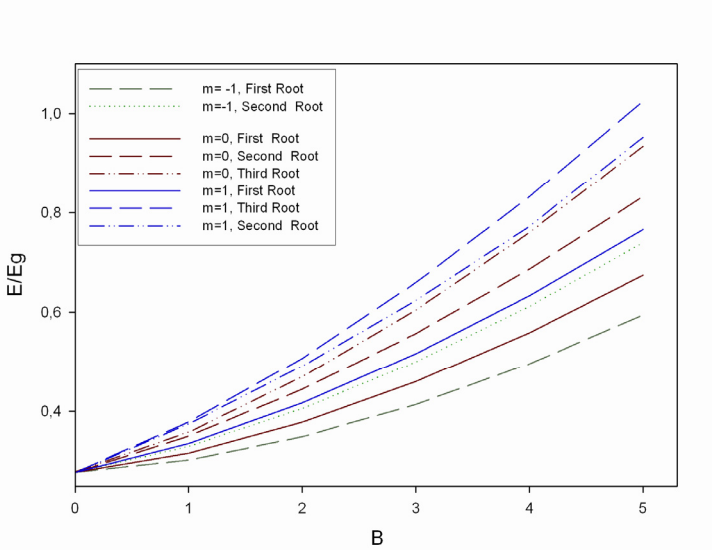

Fig. 6. Energy eigenvalues as a function of magnetic field, for different (n, m) states.

In Figure 6, it's shown the magnetic field dependence of the subbands for different n and different m values for electrons in InSb quantum anti-wire, where the radius and height is taken as 300 Å and 200 Å respectively. The presence of the inner forbidden region for the electron's motion as well as the confining potential of the anti-wire also leads to a sequence of the ground state energy subbands so that the lowest m(0,0) subband is no longer always the ground state. It's clearly seen from the Figure 6 that the ground state is m(0,-1) while it was m(0,0) for the quantum-wire. The ground state expects the $-|m|$ energy subband for which the electron's cyclotron motion is least constrained by the walls of the confining potential of the quantum anti-wire.

3. Conclusion

The energy eigenvalues of a single electron confined near a cylindrical cavity of a Kane type semiconductor quantum disk have been obtained theoretically in presence of Rashba spin–orbital interaction. The simple parabolic band model is used to describe electrons in weak Rashba spin–orbit coupling regimes. We calculated the radii, height, coupling strength, and magnetic field dependence of Rashba splitting for electrons. It has been seen that the Rashba splitting of the electrons are decreased with the increasing of radius.

References

[1] Chakraborty T 1999 Quantum Dots (Amsterdam: Elsevier)
[2] Rashba E I Sov. Phys. Solid State 2, 1109 (1960).
[3] Dresselhaus G Phys. Rev. **100**, 580 (1955).
[4] Dyakonov M I and Perel V I Zh. Eksp. Teor. Fiz. **60**, 1954 (1971).
[5] Data S and Das B Appl. Phys. Lett. **56**, 665 (1990).
[6] Ohkawa F. Uemura Y J. Phys. Soc. Jpn. **37**, 1325 (1974).
[7] Lassnig R Phys. Rev. B **31** 8076 (1985).
[8] Pfeffer P and Zawadzki W Semiconductor Science Technology **19**, R1-R17 (2004).
[9] Tsitsishvili E, Lozano G S and Gogolin A O Phys. Rev. B **70**, 115316 (2004).
[10] Bulgakov E N, Sadreev A F Pis'ma Zhetf **73**, 10 (2001).
[11] Hashimzade F M, Babayev A M, Çakmak S, Çakmaktepe S Physica E: "Lowdimensional Systems and Nanostructures **25(**1) 78-85 (2004).
[12] Kudryashov V V Math-Ph. **2** 0708.3904 (2007)
[13] Reijniers J, Peeters F M, Matulis A Phys. Rev. **B 59,** 2817 (1999).

[14] Lourtioz J M Photonic Crystals (Berlin Heidelberg: Springer Verlag) p.507, 2008.
[15] Ozbay E, Guven K, Aydin K, Bayindir M International Journal of Nanotechnology **1**(4) 379 – 398 (2004).
[16] Destefani C F, Ulloa S E and a)b)c)d)Marques G E Phys. Rev. B **69**, 125302 (2004)

*Corresponding author: cakmaktepe2001@yahoo.com